Intrinsic surface band bending in $Cu_3N(100)$ ultrathin films

C. Navío,[1,*] M. J. Capitán,[2] J. Álvarez,[1] F. Yndurain,[1] and R. Miranda[1]
[1]*Departamento de Física de la Materia Condensada e Instituto de Ciencia de Materiales Nicolás Cabrera, Universidad Autónoma de Madrid, Cantoblanco, 28049 Madrid, Spain*
[2]*Instituto de Estructura de la Materia-CSIC, c/Serrano 119, 28006 Madrid, Spain*
(Received 8 March 2007; revised manuscript received 31 May 2007; published 6 August 2007)

Highly homogeneous, ultrathin films of copper nitride (Cu_3N) have been grown on Fe(001) at room temperature using a Cu evaporator and a radio-frequency plasma source to obtain atomic nitrogen in a UHV environment. Cu_3N is a semiconductor with the valence band edge at -0.65 ± 0.05 eV below the Fermi Level. The formation of copper nitride can be detected spectroscopically by the shape of the Cu LVV-Auger electron transition, which changes sensibly in shape and position compared to metallic Cu. Cu_3N grows epitaxially with the substrate forming flat disklike mosaic blocks, (001) oriented. Both x-ray core level photoelectron spectroscopy and ultraviolet photoelectron spectroscopy photoemission experiments have been used to study the electronic structure. A first-principles calculation has been performed and compared with the measured spectra.

DOI: 10.1103/PhysRevB.76.085105 PACS number(s): 68.55.−a, 73.20.At, 61.10.−i

I. INTRODUCTION

Cu_3N is a semiconducting material that is attracting increasing interest for several areas of application. It is stable at 300 K, but thick films decompose at 700 K, which has been employed for maskless writing of microscopic metallic contacts[1] or write-once optical recording.[2–5] It has also been proposed that all-nitride, epitaxial, single crystal magnetic tunnel junctions consisting of $Fe_4N/Cu_3N/Fe_4N$ can be prepared simply by alternate evaporation of Fe and Cu in a flux of highly reactive N atoms.[6] This idea benefits from the fact that some iron nitrides [Fe_4N (Refs. 7–9) and $Fe_{16}N_2$ (Refs. 10 and 11)] are low-resistance, high magnetization magnetic materials with a cubic structure that can be grown epitaxially as single crystals on different substrates.[12–14] The moderate insulating character of Cu_3N and its capability to create nanostructures have been being recently used to decouple Cu islands and Mn atoms from a Cu substrate and study the surface state, size-dependent shift due to confinement[15] or the low energy spin excitations of antiferromagnetic chains,[16] respectively.

Cu_3N has a rather open cubic crystalline structure and a lattice parameter of $a_{\gamma\text{-}Cu_3N}=3.815$ Å. Its structure is built up from rigid perpendicular Cu-N-Cu bonds and it is compatible with surfaces and/or interfaces ending in either pure copper planes or mixed copper-nitrogen planes. The mixed copper-nitrogen plane can be visualized as a sort of solid state equivalent of the transition metal-nitrogen ring in porphyrins, a group of molecules that are candidates for molecular-based electronic components such as memory devices.[17] It is well established that the optical and transport properties change dramatically with the sequence of stacking of the porphyrins.[18] Cu_3N is, thus, particularly interesting as a substrate for the growth of single crystals of porphyrins on semiconductors. Additionally, the development of hybrid inorganic-organic solar cells has opened the interest in using Cu_3N nanoparticles bonded to suitable organic donor and/or acceptor molecules. The surface interaction between Cu_3N and organic molecules is basically unknown.

In spite of its potential interest, the electronic structure of Cu_3N in bulk and in surfaces is not well known, and its capability to be grown epitaxially has nor been demonstrated. Previous theoretical calculations predict a band gap of either 0.23 eV (using linear augmented plane wave[19]) or 0.9 eV (using linear combination of atomic orbitals).[20] The gaps determined experimentally are generally larger but vary widely from 0.8 to 1.9 eV.[3,4,6] This could indicate that the actual composition and microstructure of the material and, thus, its band gap depend on the experimental conditions. In fact, sub- and overstoichiometries for Cu_3N films prepared by sputtering have been reported to decrease the observed band gap.

We report here the growth of homogeneous films of $Cu_3N(100)$ on Fe(001) even at nanometer thickness. We describe an experimental characterization of the electronic structure of the $Cu_3N(100)$ surface by ultraviolet photoelectron spectroscopy (UPS) and x-ray core level photoelectron spectroscopy (XPS) and the corresponding first-principles calculation of the electronic structure and their comparison.

II. EXPERIMENTAL AND THEORETICAL METHODS

The films have been grown in an ultrahigh vacuum chamber, with a base pressure of 3×10^{-10} mbar. The Fe(001) substrate was chosen to characterize possible reactions involving transfer of N to the substrate during growth or thermal processing, a point difficult to verify if an iron nitride substrate is used. The result shows that there is diffusion of N into the Fe substrate inducing a significant change in the magnetic properties. This results should be described elsewhere.[21] The Fe(001) crystal was cleaned by repeated cycles of Ar^+ bombardment (1 keV) and annealing up to 920 K until no contamination (O and C) was detected by XPS or Auger electron spectroscopy.

For the growth of copper nitride thin films, we used a flux of atomic Cu from a standard metal evaporator and a radio-frequency plasma discharge as a source of atomic nitrogen.[12] The efficiency in the production of atomic N is 15% in the experimental conditions used. This nitrogen source facilitates the nitride formation as demonstrated in the epitaxial growth of iron nitrides.[8,12] The growth was carried out at room tem-

TABLE I. Thickness and stoichiometry for different copper nitride thin films. The films are denoted as $A\,Cu_XN$, where A increases with the film thickness.

Name	$d_{\lambda_{Cu}}$ (Å)[a]	$d_{\lambda_{Cu_3N}}$ (Å)[a]	Chemical composition Cu $2p_{3/2}$/total N 1*s*
$1Cu_3N$	5	7	0.7
$2Cu_3N$	27 (43)	41	2.2
$3Cu_3N$	30	45	2.3
$4Cu_3N$	42 (63)	63	2.7
$5Cu_3N$	⩾60	⩾80	2.7

[a]The film thickness was calculated by the attenuation of the Fe $2p$ peak of the substrate by the deposited copper nitride thickness (d), as given by $I_{Fe}=I_{Fe}^{\infty}e^{-d/(-\lambda_{Cu-N})}$, with I_{Fe} and I_{Fe}^{∞} being the Fe peak intensities of the deposited sample and the substrate, respectively, and λ_{Cu-N} the mean free path of an electron with Fe_{2p} kinetic energy in Cu_3N. Results in column 2 were obtained with the tabulated value for Cu (10.7 Å), and results in column 3 were obtained with the value (16 Å) from fits to the thickness calculated from the x-ray reflectivity patterns (in parentheses in column 2)

perature. During the film growth, the pressure in the chamber was 5×10^{-7} mbar, but only nitrogen was detected by the residual gas analyzer. Homogeneous, ultrathin Cu_3N films, down to 1 nm thickness, were formed on the Fe(001) surface with this method.

The chemical characterization and the determination of the stoichiometry and the thickness of the grown films were carried out by XPS ($h\nu$(Mg $K\alpha$)=1253.6 eV) using a hemispherical analyzer Leybold-Heraeus (LHS10) to detect the ejected electrons. The photon energies used for UPS were 21.22 eV (He I) and 40.8 eV (He II). Data from different samples are presented in this work. Their notation is ACu_3N, where A is an integer number that increases with the film thickness (see Table I for correspondence).

The structural characterization of the films have been performed by means of *in situ* low energy electron diffraction (LEED) and *ex situ* x-Ray diffraction (XRD), using a six-circle diffractometer with optimized geometry for surface analysis placed on a rotatory anode, which produces Cu $K\alpha$ (8040 eV) radiation. The incoming beam size was defined by combining two collimating presample slits separated by 250 mm. The diffracted beam was detected by using a scintillator NaI detector and combined with a graphite analyzer and two postsample slits giving good energy and reciprocal space resolution. The dynamic range of the detector was increased to detect both the Bragg peaks coming from the substrate and those corresponding to the thin film compounds with the same diffractometer configuration, by using the "automatic attenuator system" described elsewhere.[22]

The experimental results were compared with first-principles theoretical calculations performed in the context of density functional theory[23] using the SIESTA[24] method. For the exchange correlation potential, we adopt a generalized gradient approximation.[25] The norm conserving pseudopotentials used follow the Troullier-Martins scheme[26] in the nonlocal form proposed by Kleinman and Bylander[27] and with partial core corrections.

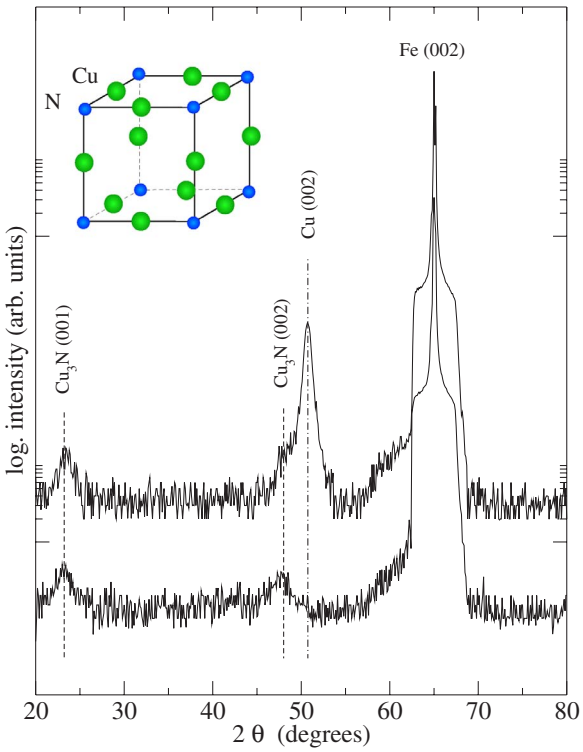

FIG. 1. (Color online) X-ray diffraction pattern for a 63-Å-thick Cu_3N film as deposited (lower curve) and for a 41-Å-thick Cu_3N film capped by 230±10 Å of Cu and heated to 370 K (upper curve). The inset shows the bulk crystalline structure of Cu_3N. The small (blue) spheres are N atoms and the large (green) are Cu atoms.

III. RESULTS AND DISCUSSION

A. X-ray diffraction

Cu_3N has a cubic, anti-ReO_3 crystalline structure, which is reproduced in the inset of Fig. 1. It has a lattice parameter of $a=3.83\pm0.02$ Å. The structure and crystalline quality of the films were examined by means of *ex situ* XRD and x-ray reflectivity. Figure 1 shows specular, wide angle 2θ scans for two films (capped and uncapped) with the intensities plotted in logarithmic scale. The prominent Fe(002) reflection corresponds to the substrate, while the other Bragg peaks at lower angle correspond to epitaxial cubic $Cu_3N\{001\}$. The upper curve shows, in addition, the Cu(002) reflection of the Cu capping layer. There are no changes in the shape or additional peaks in the unprotected film (lower curve), which indicates that Cu_3N is stable in air.[1] The width of the specular Bragg peaks reflects the size of the mosaic blocks along the direction perpendicular to the film. The full width at half maximum (FWHM) of the $Cu_3N(001)$ reflections corresponds to a block mosaic size of 46±6 Å, which is similar to the film thickness (see Table I).

Figure 2 shows with open circles a representative x-ray reflectivity measurement for a copper nitride film. The reflectivity gives information about the morphological roughness, electronic density, and thickness of the film.[28] The slow intensity decay and the oscillation shape indicate a mean square surface roughness of the film of 4±1 Å, i.e., equivalent to the one of the Fe(001) substrate. This means that the

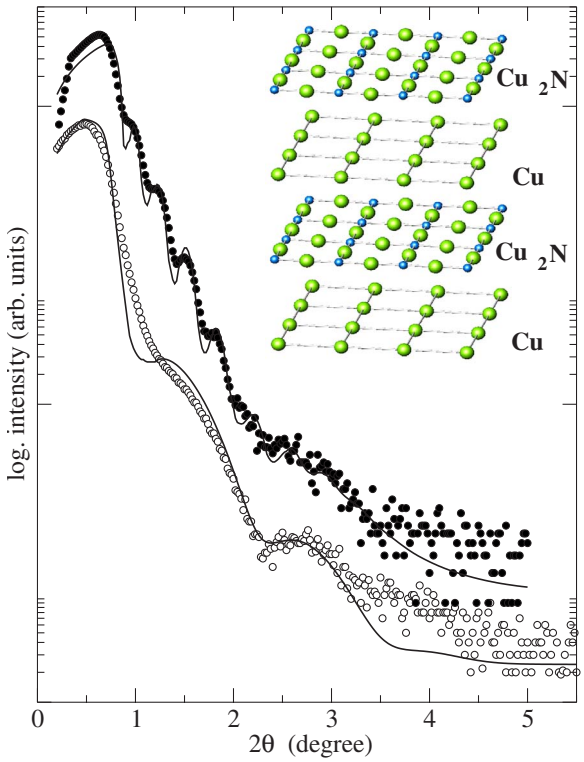

FIG. 2. (Color online) Measured x-ray reflectivity diagrams for two representative Cu_3N samples: 63 Å thick (open dots) and 41 Å thick (filled dots). The latter was covered with a protective Cu film of 230±10 Å and heated to 370 K. The corresponding fits are shown as continuous lines. The inset shows the layer-resolved structure of $Cu_3N(100)$.

surface roughness is not increased by the method of growth of the nitride. The continuous line represents the reflectivity curve calculated for a Cu_3N film thickness of 63±4 Å. Figure 2 also compares the measured diagram (filled circles) with the calculated one for a 43±4 Å thick copper nitride film (denoted as $2Cu_3N$) protected with a 230±10 Å Cu capping layer. The deep reflectivity oscillations indicate that the Cu capping does not modify noticeably the surface roughness.

The in-plane orientation of the film was checked by means of ϕ-pole x-ray scans with the outgoing angle (2θ) fixed at the corresponding (111) Bragg peak of $Cu_3N(001)$. The results are presented in Fig. 3, which shows four well defined Bragg peaks separated by 90°. This indicates that the crystals grow with the in-plane symmetry imposed by the substrate, i.e., they are epitaxial and oriented in plane. The (111) direction of the $Cu_3N(001)$ crystals is rotated 45° within the surface plane with respect to the one corresponding to the Fe substrate. This rotation allows a reasonable matching of the atomic distances in the film plane between both materials.[29] The FWHM of the (111) Bragg peak of the $Cu_3N(001)$ crystals indicates that these crystals have an average lateral size of 50±20 Å in the film plane. The epitaxial growth and the small crystallites size are also reflected in the LEED pattern obtained for $Cu_3N(001)$ grown on Fe(001), as shown in the inset of Fig. 3.

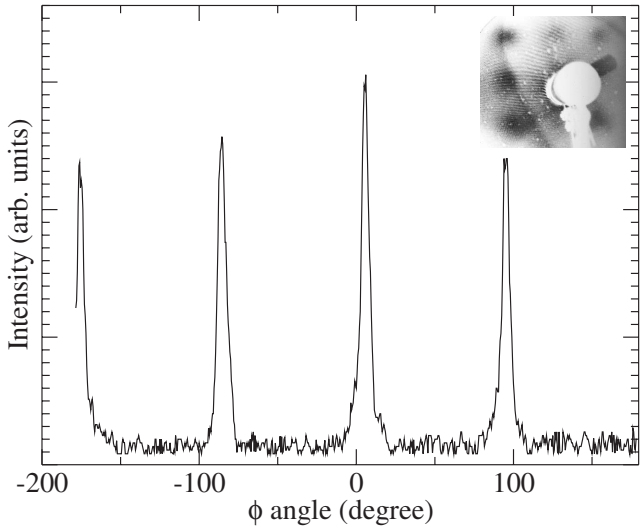

FIG. 3. In-plane scan at the (111) Bragg peak for 63 Å-thick Cu_3N film, assuming that the Cu_3N nanocrystals are oriented with the (001) direction along the perpendicular to the surface. The inset shows the LEED pattern. Notice the broad spots indicative of a small lateral size of the crystallites.

B. Photoemission (x-ray core level photoelectron spectroscopy and ultraviolet photoelectron spectroscopy)

The upper panel of Fig. 4 shows the Cu $2p$ photoemission peaks for a 5-nm-thick copper nitride film (denoted as $3Cu_3N$) and for Cu(001). The Cu $2p$ peak of the copper nitride film is shifted 0.5±0.1 eV to higher binding energy (BE), but the shape is not changed with respect to metallic Cu. A similar chemical shift has been observed by other authors.[30]

The presence of N in the film is testified by the appearance of a photoemission peak in the N $1s$ energy region (see lower panel of Fig. 4). This indicates that the Cu $2p$ energy shift is due to the formation of a copper nitride compound. The N $1s$ peak has two components: a main peak at 398.7 eV and a shoulder shifted 1.0±0.1 eV to lower BE. Both components are observed in all nitride films grown, and the absolute intensity of the shoulder is almost constant in all the studied samples. Both values are almost identical to the ones measured in the same conditions for $Fe_4N(100)$.[14] Accordingly, the larger peak at 398.7 eV is ascribed to N in the bulk of Cu_3N, while the one at 397.7 eV is assigned to N adsorbed at the surface of $Cu_3N(100)$. This is also in agreement with previous observations for N atoms adsorbed on many transition metal single crystal surfaces.[14,31–33] Contrary to previous reports,[33] the peak at 397.7 eV cannot be assigned to adsorbed NO, since no O was detected in our case by either XPS or Auger. The assignment of the shoulder to surface N would also explain that the absolute area of the shoulder does not decrease with the film thickness.

The formation of a Cu-N compound is also dramatically reflected in the energy region corresponding to the Cu LVV-Auger transitions (Fig. 5). The spectrum of the film shows a clear shift to lower kinetic energies (2.0±0.1 eV) of the main peak and the disappearance of two additional features. This

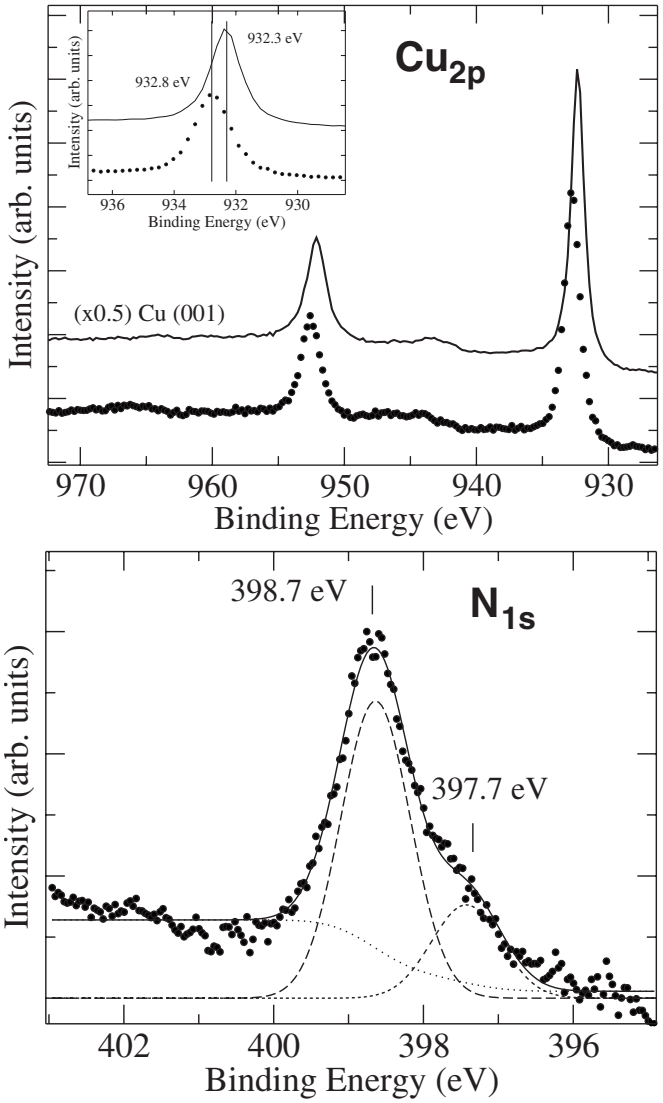

FIG. 4. Upper panel: Cu $2p$ photoemission spectra of a 45-Å-thick Cu_3N (points) and Cu(001) (continuous line). The inset shows the Cu $2p3/2$ core level shift. Lower panel: N $1s$ photoemission energy region for a 45-Å-thick Cu_3N film (points) and its fit (continuous line) considering two components (dashed lines) and a background.

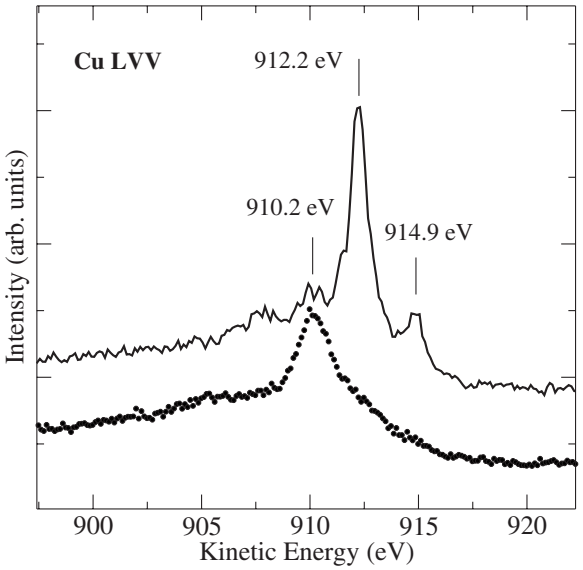

FIG. 5. X-ray excited LVV-Auger spectra for a 45-Å-thick $Cu_3N(100)$ film deposited on Fe(100) (points) and for Cu(100) (continuous line).

reflects the changes in the density of states (DOS) of the valence band upon nitride formation. The shape of the Auger peak can be used as a fingerprint of the formation of the Cu_3N compound.

The Cu $2p$ and N $1s$ core level peaks, after subtraction of the background, were fitted with standard line shapes.[34] The ratio of the Cu $2p_{3/2}$ and N $1s$ peak areas can be used to determine the average atomic composition of the films following standard procedures[35] and using the atomic sensitivities determined previously for this particular spectrometer.[36] The thinnest film has a much higher apparent N content, mostly due to the large amount of N bonded to the Fe substrate.[21] Considering the enrichment of N at the Cu/Fe interface, the resulting stoichiometry is $Cu_{2.7\pm0.3}N$ for the rest of films. The stoichiometry obtained for the two thicker films (4 and 5) is closer to the bulk one because the thickness is larger than the escape depth of photoelectrons, rendering the surface contribution negligible.

Assuming that the films are strictly homogeneous within the escape depth of the electrons, the ratio of the intensities of the Cu $2p_{3/2}$ and N $1s$ peaks is related to the atomic density ratio (X_{Cu}/X_N) by

$$\frac{X_{Cu}}{X_N} = A\frac{I(Cu_{2p})}{I(N_{1s})}, \tag{1}$$

where

$$A = \frac{1/S_{Cu}}{1/S_N} \tag{2}$$

and S_{Cu} and S_N are the atomic sensitivity factors determined for the pure chemical elements for the specific electron analyzer used.[36] The chemical composition of different films, calculated using the total area of the N $1s$ peak, is shown in the last column of Table I. The average stoichiometry of the copper nitride films is 2.5 ± 0.2 Cu per N atoms with the exception of the thinnest film. For this calculation, both N $1s$ components are taken into account. The higher stability of the surface ending in the mixed Cu-N plane and the exponential decay of the XPS sensitivity away from the surface overestimate the N signal with respect to bulk Cu_3N. This effect is more pronounced for films with a thickness smaller than the analysis depth of XPS. Thus, the apparent stoichiometry evolves from 2.2 to 2.7 for the thickest sample.

The anti-ReO type of crystalline structure of Cu_3N can be described as a lattice of fcc Cu with 1/3 (top/bottom) of copper cube face missing and with the nitrogen atoms occupying the octahedral edge places. Such structure is stable within a small composition range region around Cu_3N. Thus, the final structure is formed by alternatively stacking planes containing Cu/N in a 2/1 ratio and pure Cu (with a density half of the one of a Cu fcc layer). The theoretical calculations

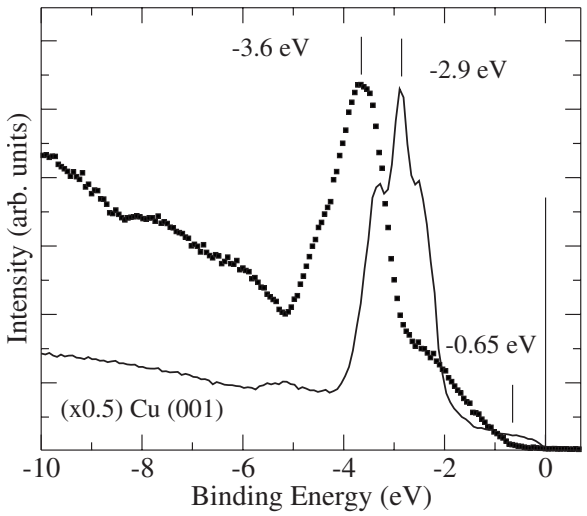

FIG. 6. He I UPS spectrum of a 45-Å-thick $Cu_3N(100)$ film (dots) compared to Cu(001) (continuous line).

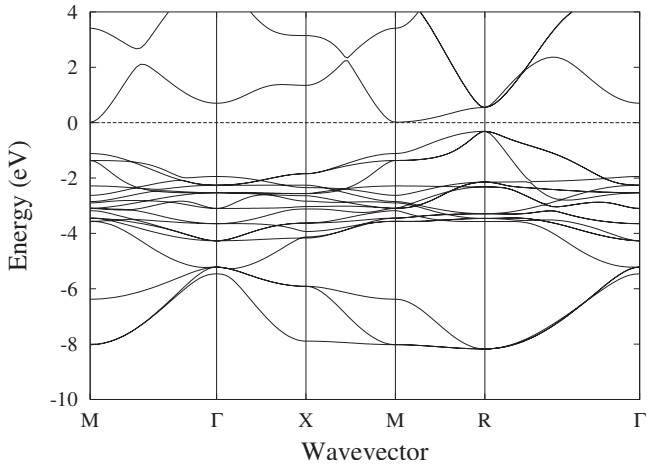

FIG. 7. Calculated band structure of Cu_3N along the main symmetry directions. The energy origin is at the Fermi level.

give that the structure ending on the copper nitride layer is 1.6 eV per surface unit cell more stable than the corresponding ending on the pure copper layer. These data are in agreement with the assumption that the appearing higher binding energy N 1*s* XPS peak can be assigned to the surface nitrogen.

In Fig. 6, we show the He I UPS spectra of $Cu_3N(100)$ thin film and Cu(001). First, we notice a relative shift for the main peak of the Cu *d* band of Cu_3N by 0.7 eV to higher BE. Second, in the Cu_3N case, there is a lack of electron emission at the Fermi level confirming its semiconducting character with the valence band edge located 0.65 ± 0.05 eV below the Fermi level. The valence band edge position is the same for all the nitride films independent of their thickness. This value represents a lower bound for the band gap, and it is compatible with the experimental values reported in the literature[3,4,6] for the Cu_3N band gap (from 0.8 to 1.9 eV) and for the optical gap for indirect transitions [1.24 eV (Ref. 37)].

For a complete analysis of the electronic structure of the Cu_3N films, we have performed a first-principles calculation using the SIESTA code.[24] For the crystalline structure, we obtain an equilibrium lattice constant of 3.88 Å, 1.3% larger than the experimental one (3.83 Å). Figure 7 shows the calculated bulk band structure for the experimental lattice constant. The bands agree with previous results obtained using a different method of calculation based on plane waves.[19] We obtain a semiconductor with an indirect absolute gap of 0.32 eV and direct gaps of 1.09 and 0.87 eV at the Γ and *R* points, respectively. The indirect gap is much smaller than the observed valence band edge (see Fig. 7), as one would expect for density functional theory calculations, which systematically underestimate band gaps.

In order to calculate the surface electronic structure of Cu_3N, slabs of different thicknesses were considered and the convergence of the relevant precision parameters was carefully checked. The calculations were such that, starting with the ideal geometry and the theoretical lattice constant of 3.88 Å, the atomic geometry at the surface were relaxed until the force on the atoms was below 0.02 eV/Å. Then, the found equilibrium geometry was rescaled by a 1.3% factor to recover the experimental lattice constant for the inner layers of the slab. Out of the two possible surface terminations, namely, Cu_2N and pure Cu, we only considered the former one since its energy formation is 1.6 eV per surface unit cell lower than the latter. We have then calculated the local densities of states (LDOSs) for the different layers in the vicinity of the surface.

The layer-resolved LDOSs calculated for an 11 layer slab of Cu_3N are shown in Fig. 8. The bulk DOS is dominated by the *d*-derived peak centered at −4.5 eV. There is a characteristic feature at −3 eV, not present in Cu(100), and weaker features around −7.5 and −9.5 eV due to the Cu-N bonds. The bulk DOS is similar to the LDOS at one the Cu_2N planes (see, e.g., S-2 in Fig. 8). Notice that the LDOS of the two layers closer to the surface (S-1 and S) is shifted 0.7 eV to lower BE with respect to the bulk. Thus, the theoretical calculations indicate that there is a surface band bending (upward) that extends around 1 nm inside the film. The origin of the band bending can be traced in the calculations to a decrease of the total charge in the second topmost layer (S-1) of the order of 0.1 electron/Cu atom. The UPS spectrum shown in the upper curve of Fig. 8 reflects essentially the LDOS at the surface. There is an overall agreement between theory and measurements. The main structures of the UPS spectrum are reproduced in the calculation. It is worth noticing that the hump observed around −10 eV is due to the layers underneath and not to the topmost one. The experimental spectrum contains contributions of the shifted LDOS of the layers underneath the surface, which broaden the features and explain the lower resolution of the Cu_3N spectrum as compared with the one of Cu(100) shown both in Fig. 6.

This theoretical prediction is confirmed by the XPS core level data. The upper panels of Fig. 9 show that the Cu 2*p* and N 1*s* peak positions depend on the thickness of the film. The peaks shift to larger BEs for increasing film thickness following an exponential law with a maximum shift of

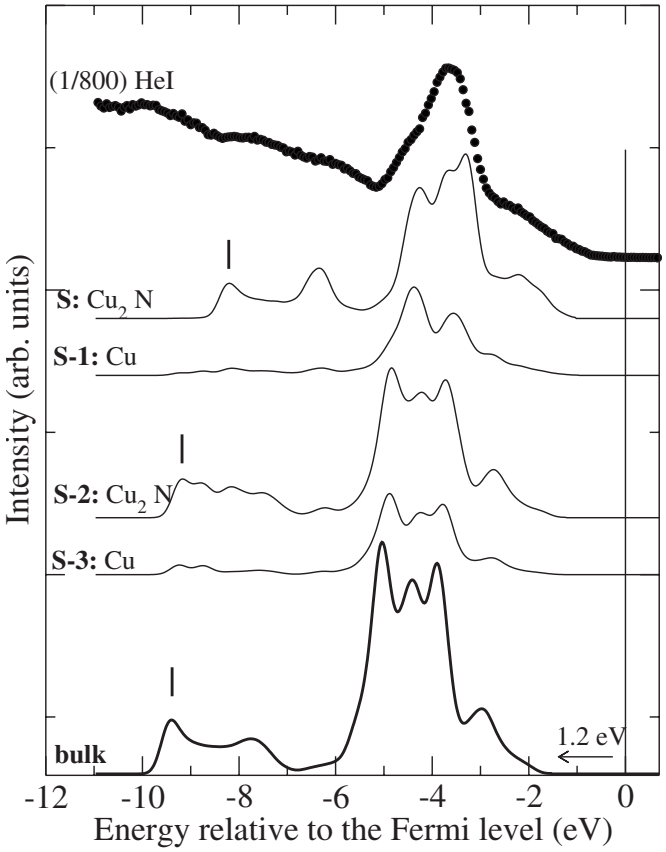

FIG. 8. Layer-resolved local density of States calculated for an 11 layer $Cu_3N(100)$ slab. The upper curve shows the UPS spectrum of $Cu_3N(100)$. The thin lines reproduce the calculated LDOS for different layers close to the surface (S). A small energy broadening has been included in the calculated curves to compare with the experimental spectra. The calculated curves have been shifted 1.2 eV (in the direction indicated by the arrow).

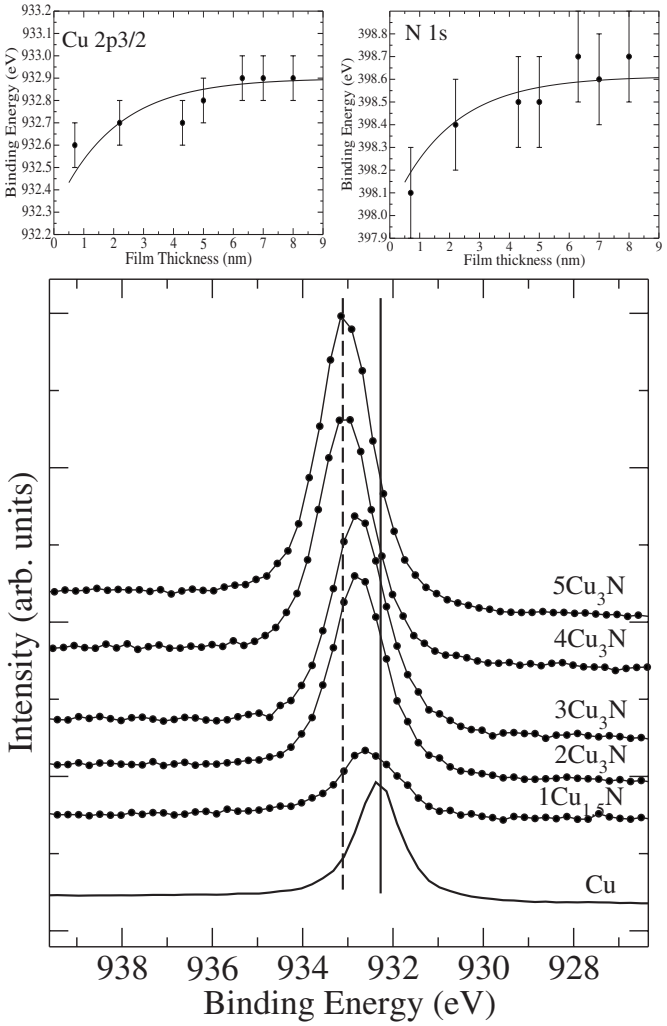

FIG. 9. Upper panels: Energy position of the Cu $2p3/2$ and N $1s$ core levels as a function of the thickness of the Cu_3N films. Lower panel: Cu $2p3/2$ photoemission spectra for Cu_3N films of increasing thickness. The continuous line indicates the peak position for Cu(001), while the dashed line corresponds to the measured position for the thicker Cu_3N film.

0.6 eV and a characteristic depth of 2 nm. The FWHM of the Cu $2p_{3/2}$ photoemission spectrum remains constant. Thus, the shift cannot be explained by the contribution of different Cu $2p_{3/2}$ components. Furthermore, the stoichiometry of the films remains constant as shown by XPS. Therefore, we assign the energy shift observed with the Cu_3N film thickness to the band bending effect, suggested by our theoretical calculations.

Soto *et al.*[30] found also a chemical shift in both the Cu $2p$ and the N $1s$ toward lower binding energy by increasing the partial pressure of nitrogen during the copper nitride formation by means of pulsed laser deposition. In that case, the chemical shift was related to the formation of sub- and overstoichiometry Cu_3N films.

Figure 10 shows schematically the band structure of Cu_3N (100) around the Fermi energy, including band bending and the band gap. From the measured valence band edge at the surface (0.65 eV, see Fig. 6) and the band bending obtained from the Cu and N core level shifts (0.6 eV, see Fig. 9), the position of the Fermi level in the bulk of Cu_3N can be calculated to be 1.25 eV above the valence band edge. Thus, the band gap for Cu_3N is, at least, 1.25 eV, which is very close to the reported gap for optical indirect transitions of 1.24–1.3 eV.[2] This result further indicates that the Fermi level is close to the conduction band edge, suggesting that it is a *n*-type semiconductor. This *n*-type behavior can be intrinsic to Cu_3N (100), i.e., not due to external doping by impurities, since there is a strong asymmetry in the valence and conduction band DOSs. According to our first-principles calculations for the intrinsic material, the DOS in the valence band is much larger than in the conduction band, setting the Fermi level close to the conduction band in the bulk. The lower electronic density in the Cu layer just below the surface originates the upward bending of the bands at the (100) surface. Other possible origin of the Cu $2p$ core level shift such as initial state (interaction with the substrate) and final state (relaxation) effects induced by the metal substrate has

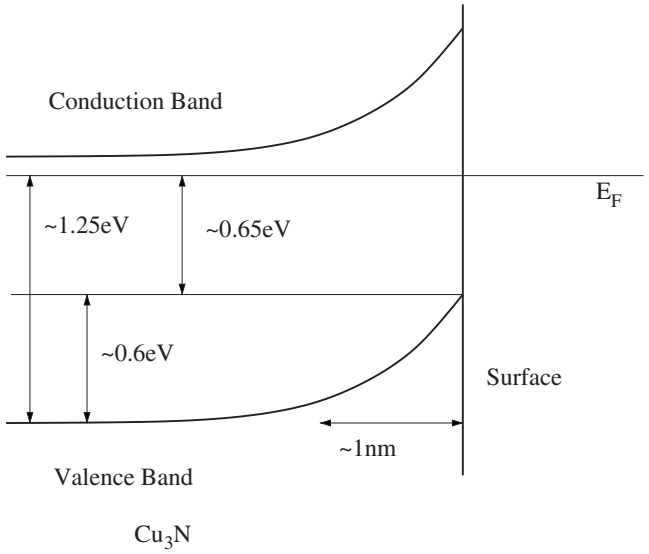

FIG. 10. Schematic diagram of the relevant electronic levels in a Cu_3N (100) film.

been considered and rejected for the following reasons: Upon increasing the Cu_3N thickness, a decreasing relaxation of the Cu $2p$ core hole shielding by the electrons of the metallic substrate could lead to a shift toward higher BEs, as observed, but the electron density in degenerate, n-type, small gap Cu_3N is similar to the one of the Fe substrate and the corresponding relaxation is expected to be almost identical.[38] The charge transfer between Cu atoms and the Fe substrate is negligible, as indicated by calculations for $Fe_4N/Cu(100)$,[13] and, thus, initial state (chemical) shifts are not expected to play a role in this system.

In order to ascertain the role of impurities in the surface bending, we have studied the stability of different impurities at the surface vicinity. We have considered interstitial atomic oxygen and nitrogen. The impurities are placed at an initial position either in the Cu plane under the topmost Cu_2N layer or above it, and the atomic forces acting on the atom are calculated. Then, the atom is moved to its next position using a conjugated gradient technique. The process is followed until the forces in the atoms are smaller than 0.02 eV/Å. Figure 11(a) shows the results for a N atom placed initially either below or above the surface. In both cases, the atom finally sits on top of the surface. This behavior is opposite to the one observed in $Fe_4N(100)$, where the excess N remains under the surface, stabilizing the surface reconstruction.[13] The case of an oxygen atom is represented in Fig. 11(b). We find that interstitial oxygen diffuses away from the surface plane toward the bulk. These calculations stress the high chemical stability of the $Cu_3N(100)$ surface.

IV. CONCLUSIONS

It is possible to grow ultrathin films of Cu_3N onto Fe(001) single crystal down to nanometer thickness. The films are reasonably flat and exhibit semiconductor behavior with the valence band edge at 0.65 ± 0.05 eV below the Fermi level independent of their thickness. The LVV-Auger spectrum can

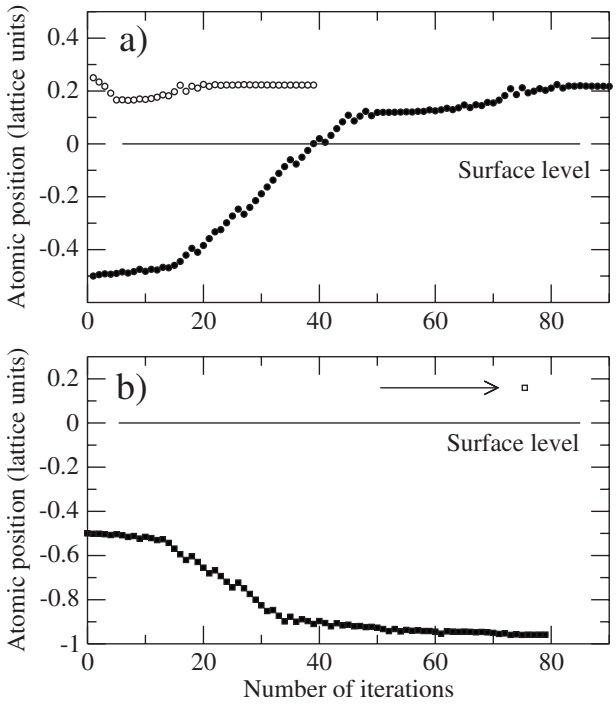

FIG. 11. Position with respect to the surface plane calculated for (a) nitrogen and (b) oxygen interstitial atoms located initially close to the surface layer of Cu_3N (100). The x axis corresponds to the number of iterations. The zero level is at the surface. Positive values correspond to the vacuum side and negative to the Cu_3N film. The arrow in (b) indicates the calculated final position for oxygen on top.

be used as a fingerprint of the formation of the copper nitride. The films deposited at 300 K consist in relatively large mosaic blocks of Cu_3N crystals oriented with the (001) direction along the Fe(001) single crystal direction.

We have also shown that the photoemission techniques combined with x-ray diffraction are very complementary techniques in characterizing the electronic and atomic structures of the deposited film. Thus, it has been possible to determine the mean free path of the Fe $2p$ electrons in the copper nitride material.

It has been shown that a characteristic feature of the copper nitride compound is the the LVV-Auger spectrum which suffers a noticeable change not only in position but also in shape, becoming a good fingerprint of the copper nitride formation.

The Cu $2p$ photoemission peak of the copper nitride shifts with respect to the copper metal from 0.3 to 0.9 eV for the studied samples (from 1 to 8 nm thick), which is in the range observed by other authors (0.8 eV).[30] It has been shown that in the studied samples, the composition is constant except for the thinnest sample ($1Cu_3N$).

The first-principles electronic structure calculations have helped in a better understanding of the system. Three main results can be pointed out: First, the theoretical calculation gives that the structure ending on a copper nitride layer is more stable than the corresponding one ending on a pure Cu layer. Second, the layer-resolved DOS indicates that there is

a band bending which is at the origin of the XPS peak shift with the film thickness experimentally observed. Thus, a lower bound for the experimental band gap is 1.25 eV. Third, the study of the impurities at the surface vicinity indicates that the N atoms tend to leave the copper nitride bulk, resulting in a behavior that is clearly different from the calculated for the iron nitride film.

ACKNOWLEDGMENTS

C.N. acknowledges the Spanish Ministry of Science and Technology (FP-2001-1310). This work had the financial support of grants from both MCyT (NAN2004-08881-C02-01 and MAT2004-05865) and CM (CAM 07N/0023/2002).

*cristina.navio@uam.es

[1] M. Asano, K. Umeda, and A. Tasaki, Jpn. J. Appl. Phys., Part 1 **29**, 1985 (1990).
[2] T. Maruyama and T. Morishita, J. Appl. Phys. **78**, 4104 (1995).
[3] T. Nosaka, M. Yoshitake, A. Okamoto, S. Ogawa, and Y. Nakayama, Thin Solid Films **348**, 8 (1999); T. Nosaka, M. Yoshitake, A. Okamoto, S. Ogawa, and Y. Nakayama, Appl. Surf. Sci. **169-170**, 358 (2001).
[4] J. F. Pierson, Vacuum **66**, 59 (2002).
[5] Y. Hayashi, T. Ishikawa, and D. Shimokawa, J. Alloys Compd. **330-332**, 348 (2002).
[6] D. M. Borsa, S. Grachev, C. Presura, and D. O. Boerma, Appl. Phys. Lett. **80**, 1823 (2002).
[7] J. L. Costa-Krämer, D. M. Borsa, J. M. Garcia-Martin, M. S. Martin-Gonzales, D. O. Boerma, and F. Briones, Phys. Rev. B **69**, 144402 (2004).
[8] J. M. Gallego, S. Y. Grachev, D. M. Borsa, D. O. Boerma, D. Ecija, and R. Miranda, Phys. Rev. B **70**, 115417 (2004).
[9] D. Ecija, E. Jimenez, J. Camarero, J. M. Gallego, J. Vogel, N. Mikuszeit, N. Sacristan, and R. Miranda, J. Magn. Magn. Mater. **316**, 321 (2007).
[10] J. M. D. Coey and P. A. I. Smith, J. Magn. Magn. Mater. **200**, 405 (1999).
[11] C. Ortiz, G. Dumpich, and A. H. Morrish, Appl. Phys. Lett. **65**, 2737 (1994).
[12] S. Yu. Grachev, D. M. Borsa, and D. O. Boerma, Surf. Sci. **516**, 159 (2002).
[13] J. M. Gallego, D. O. Boerma, R. Miranda, and F. Yndurain, Phys. Rev. Lett. **95**, 136102 (2005).
[14] C. Navio, J. Alvarez, M. J. Capitan, D. Ecija, J. M. Gallego, F. Yndurain, and R. Miranda, Phys. Rev. B **75**, 125422 (2007).
[15] F. Calleja, J. J. Hinarejos, A. L. Vazquez de Parga, and R. Miranda, Eur. Phys. J. B **40**, 415 (2004).
[16] C. F. Hirjibehedin, C. P. Lutz, and A. J. Heinrich, Science **312**, 1021 (2006).
[17] Z. Liu, A. A. Yasseri, J. S. Lindsey, and D. F. Bocian, Science **302**, 1543 (2003).
[18] L. Scudiero, D. E. Barlow, and K. W. Hipps, J. Phys. Chem. B **104**, 11899 (2000).
[19] U. Hahn and W. Weber, Phys. Rev. B **53**, 12684 (1996).
[20] M. G. Moreno-Armenta, A. Martínez-Ruiz, and N. Takeuchi, Solid State Sci. **6**, 9 (2004).
[21] C. Navio, M. J. Capitan, J. Alvarez, and R. Miranda (unpublished).
[22] J. Alvarez, E. Paiser, and M. J. Capitan, Rev. Sci. Instrum. **73**, 2788 (2002).
[23] W. Kohn and L. J. Sham, Phys. Rev. **140**, A1133 (1965).
[24] J. M. Soler, E. Artacho, J. D. Gale, A. Garcia, J. Junquera1, P. Ordejon, and D. Sanchez-Portal, J. Phys.: Condens. Matter **14**, 2745 (2002).
[25] J. P. Perdew, K. Burke, and M. Ernzerhof, Phys. Rev. Lett. **77**, 3865 (1996).
[26] N. Troullier and J. L. Martins, Phys. Rev. B **43**, 1993 (1991).
[27] L. Kleinman and D. M. Bylander, Phys. Rev. Lett. **48**, 1425 (1982).
[28] L. G. Parratt, Phys. Rev. **95**, 359 (1954).
[29] The Fe-bcc lattice parameter is 2.886 Å and for the Cu_3N is 3.83 Å. The rotation in the *xy* direction of 45° produces 3.83 Å/$\sqrt{2}$=2.71 Å.
[30] G. Soto, J. Diaz, and W. de la Cruz, Mater. Lett. **57**, 4130 (2003).
[31] W. Diekmann, G. Panzner, and H. J. Grabke, Surf. Sci. **218**, 507 (1989).
[32] K. Kishi and M. W. Roberts, Surf. Sci. **62**, 252 (1977).
[33] C. N. R. Rao and G. R. Rao, Surf. Sci. Rep. **13**, 221 (1991).
[34] The peaks were fitted, after subtraction of a Shirley background, with a Doniach-Sunjic combination of Lorentzian and Gaussian line shapes.
[35] M. P. Seah and W. A. Dench, Surf. Interface Anal. **1**, 2 (1979).
[36] J. Alvarez, J. J. Hinarejos, E. G. Michel, J. M. Gallego, A. L. Vazquez de Parga, J. de la Figuera, C. Ocal, and R. Miranda, Appl. Phys. Lett. **59**, 99 (1991).
[37] F. Fendrych, L. Soukup, L. Jastrabk, M. Cha, Z. Hubika, D. Chvostov, A. Tarasenko, V. Studnika, and T. Wagner, Diamond Relat. Mater. **8**, 1715 (1999).
[38] K. Karlsson, O. Nyqvist, and J. Kanski, Phys. Rev. Lett. **67**, 236 (1991).